# Escape behavior of quantum two-particle systems with Coulomb interactions

Tooru Taniguchi* and Shin-ichi Sawada
*School of Science and Technology, Kwansei Gakuin University, 2-1 Gakuen, Sanda City, Hyogo, Japan*
(Received 16 June 2010; revised manuscript received 26 November 2010; published 28 February 2011)

Quantum escapes of two particles with Coulomb interactions from a confined one-dimensional region to a semi-infinite lead are discussed by using the probability of finding all particles within the confined region, that is, the survival probability, in comparison with free particles. By taking into account the quantum effects of two identical particles, such as the Pauli exclusion principle, it is shown analytically that for two identical free fermions (bosons), the survival probability decays asymptotically in power $\sim t^{-10}$ ($\sim t^{-6}$) as a function of time $t$, although it decays in power $\sim t^{-3}$ for one free particle. On the other hand, for two particles with attractive Coulomb interactions it is shown numerically that the survival probability decays in power $\sim t^{-3}$ after a long time. Moreover, for two particles with repulsive Coulomb interactions it decays exponentially in time $\sim \exp(-\alpha t)$ with a constant $\alpha$, which is almost independent of the initial energy of particles.

DOI: 10.1103/PhysRevE.83.026208 PACS number(s): 05.45.Pq, 05.60.Gg, 71.10.−w

## I. INTRODUCTION

The escape is a behavior of open systems in which materials move out from an observed area. It has drawn considerable attention from various points of view, for example, Kramers' escape problem [1–3], the $\alpha$-decaying nucleus [4–6], radiative decay of molecules [7], the first-passage time problem [1–3], the recurrence time problem [8], the controlling chaos [9], and the Riemann hypothesis [10]. Escapes involve transport and can be used to calculate transport coefficients [11–13]. Particles escaping from thermal reservoirs can sustain flows such as electric currents [14,15]. Escape phenomena have been investigated in many systems, for example, billiard systems (by theories [16–18] and by experiments [19,20]), map systems [8,9,21], wave dynamics [22,23], and stochastic systems [1–3].

A typical quantity for characterizing a particle escape is the probability of finding particles within the observed area from which particles can move out, the so-called survival probability. The survival probability would decay in time because particles keep escaping from the observed area without coming back, and its decay properties have been an important subject in dynamical systems [12,13,24]. In classical billiard systems, it is conjectured, based on an ergodic argument, that the survival probability decays exponentially for chaotic systems, while it shows a power decay for nonchaotic systems [16]. This conjecture has been examined in detail, for example, in a finite-size effect of holes [17], weakness of chaos [8], a connection to correlation functions [18], and a deviation from an escape rate estimated by the natural invariant measure [8,9]. Particle escapes have also been discussed in quantum systems by using the survival probability. Reference [25] discussed an escape behavior of a free particle in a one-dimensional system, and Refs. [6], [26], and [27] investigated escapes of particle systems with a potential barrier. Quantum escapes have also been considered using a random matrix approach for quantum scattering systems [28,29] and numerical approaches to wave-packet dynamics in quantum billiard systems [30]. These studies show that the survival probability decays in power or exponentially, depending on how quantum states are superposed initially.

The principal aim of this paper is to investigate effects of particle-particle interactions in quantum escape phenomena in comparison with free-particle escapes. To investigate them in systems as simple as possible, we consider particle escapes from a confined one-dimensional region to a semi-infinite one-dimensional lead. Furthermore, as a simple many-particle system with particle-particle interactions, we choose the system consisting of two particles with Coulomb interactions and discuss interaction effects by comparing the interacting two-particle cases with the cases of one or two free particles. In these situations we consider particle escapes whose initial states are represented as an energy eigenstate of particles confined spatially in the finite region at the initial time, so that voluntariness of initial superposition of quantum states in the escape dynamics does not appear in discussions of this paper. After specifying these general setups in detail in Sec. II, we start our arguments for quantum escapes in the case of one free particle (Sec. III), in which the survival probability decays asymptotically in power $\sim t^{-3}$ as a function of time $t$. Next, we consider the cases of two identical free particles (Sec. IV), imposing quantum effects of identity of two particles, like the Pauli exclusion principle, and show analytically that the survival probability for two free bosons decays asymptotically in power $\sim t^{-6}$, while for two free identical fermions it decays asymptotically in power $\sim t^{-10}$, differently from the boson case. Then we discuss escape behaviors of two particles with Coulomb interactions (Sec. V). First, for the case of two identical fermions with attractive Coulomb interactions, it is shown numerically that the survival probability decays in power $\sim t^{-3}$ after a long time, although its power decay close to $t^{-10}$ appears for very weak Coulomb interactions. Here, the power decay $\sim t^{-3}$ of the survival probability for two-particle systems after a long time suggests that two particles are moved together like one molecule by attractive interactions, and its power decay $\sim t^{-10}$ in the weak interaction limit is consistent with the results for two identical free fermions. Second, for the case of two identical fermions with strong repulsive Coulomb interactions, we show numerically that the survival probability decays exponentially $\sim \exp(-\alpha t)$ in time with a constant $\alpha$,

*t-taniguchi@kwansei.ac.jp

 

although it decays in power close to $t^{-10}$ for very weak interactions. Our numerical results suggest that the exponential decay rate $\alpha$ of the survival probability does not depend on values of initial energies.

## II. ESCAPE OF MANY PARTICLES IN A SEMI-INFINITE ONE-DIMENSIONAL SPACE

In this paper, we consider quantum systems consisting of $N$ particles in a one-dimensional semi-infinite region $[0,+\infty)$. Before the initial time $t < 0$, we set the infinite potential barrier in the region $[l,+\infty)$ and confine the particles in the finite region $[0,l]$ with a positive constant $l$. At the initial time $t = 0$ we remove this infinite potential barrier in $x \geqslant l$, so that a particle escape to the region $[l,+\infty)$ begins to occur. The schematic illustration of this escaping behavior is shown in Fig. 1. (Here, the particles in Fig. 1 are drawn as particles with a nonzero finite size to make them visible, but in the actual models used in this paper we regard particles as material points.) To make a clear image of this kind of escape phenomena, we call the region $[0,l]$ the "subspace" and call the region $(l,+\infty)$ the "lead," so particle escape occurs from the subspace to the lead.

This system is described by the wave function $\Psi(x_1,x_2,\ldots,x_N,t)$ at time $t$ as a solution of the Schrödinger equation,

$$i\hbar\frac{\partial\Psi(x_1,x_2,\ldots,x_N,t)}{\partial t} = \hat{H}\Psi(x_1,x_2,\ldots,x_N,t), \tag{1}$$

where $\hat{H}$ is the Hamiltonian operator, $\hbar$ is the Planck constant divided by $2\pi$, and $x_j$ is the position of the $j$th particle, $j = 1,2,\ldots,N$. If the system consists of identical particles in the quantum mechanical sense, then the wave function $\Psi(x_1,x_2,\ldots,x_N,t)$ must satisfy

$$\Psi(x_1,x_2,\ldots,x_N,t) = \pm\Psi(x_1,x_2,\ldots,x_N,t)|_{(x_j,x_k)\to(x_k,x_j)} \tag{2}$$

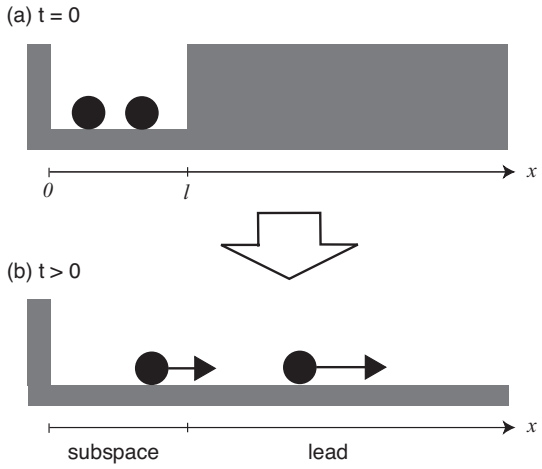


FIG. 1. Schematic of a particle escape in a semi-infinite one-dimensional system. (a) Particles confined inside a finite region $[0,l]$ at $t = 0$. (b) Particles escaping to a semi-infinite region at $t > 0$, by removing the infinite potential barrier in the region $[l,+\infty)$. In this situation we call the region $[0,l]$ the subspace and call the region $(l,+\infty)$ the lead.

for exchange of any particle indices $j$ and $k$, $j = 1,2,\ldots,N$, $k = 1,2,\ldots,N$. Here, the minus sign (plus sign) on the right-hand side of Eq. (2) should be taken for fermions (bosons) [31], for example, imposing the Pauli exclusion principle for fermions. Using the wave function $\Psi(x_1,x_2,\ldots,x_N,t)$ satisfying Eq. (1) we introduce the probability $P(t)$ defined by

$$P(t) \equiv \int_0^l dx_1 \int_0^l dx_2 \cdots \int_0^l dx_N \, |\Psi(x_1,x_2,\ldots,x_N,t)|^2. \tag{3}$$

This is the probability that the $N$ particles are still inside the subspace and have not escaped to the lead at time $t$ yet, and we call it the "survival probability" hereafter [32]. The purpose of this paper is to discuss the escape behavior of particles by a time dependence of the survival probability $P(t)$. It may be noted that the subspace can be regarded as an open system coupled to a semi-infinite lead, but the phenomena considered here are not scattering phenomena described by a response of the system to incident waves, because particles always exist only in a finite region at any finite time and the wave function is normalizable, that is, $\int_0^{+\infty} dx_1 \int_0^{+\infty} dx_2 \cdots \int_0^{+\infty} dx_N \, |\Psi(x_1,x_2,\ldots,x_N,t)|^2 = 1$ at any time $t$, different from scattering states including an incoming plain wave from the infinite region.

In general, the survival probability $P(t)$ depends on the initial condition. As an initial condition at time $t = 0$, in this paper we choose an energy eigenstate $\Phi_n(x_1,x_2,\ldots,x_N)$ of $N$ particles confined inside the subspace region $[0,l]$ corresponding to energy eigenvalue $E_n$ ($E_1 \leqslant E_2 \leqslant \cdots$). In this way, we obtain the survival probability for each initial wave function $\Psi(x_1,x_2,\ldots,x_N,0) = \Phi_n(x_1,x_2,\ldots,x_N)$ and present it as $P_n(t)$, $n = 1,2,\ldots$.

Under such initial conditions, we calculate the survival probability $P_n(t)$ analytically for free particle cases in Secs. III and IV. We also show numerical results for the survival probability by discretizing space and time in the Schrödinger equation for two-particle systems in Sec. V, as well as for part of a one-particle case in Sec. III. As a numerical technique we use the pseudospectral method [33,34]. As an example, in Appendix A we outline a spatial discretization of the Schrödinger equation for two-particle cases and its time discretization by the pseudospectral method, which are used to calculate the numerical results reported in this paper. In these numerical calculations we take the unit of $m = 1$ for the particle mass, $l = 1$ for the length of the subspace, and $\hbar = 1$ for the Planck constant divided by $2\pi$. For numerical calculations the one-dimensional space is discretized by the length $\delta x = l/\mathcal{N}_0$ with the integer site number $\mathcal{N}_0$ of the subspace (see Appendix A 1). For numerical calculations by the pseudospectral method, we also discretize the time by $\delta t$ (see Appendix A 2) and choose the concrete value of $\delta t$ so that the average energy and the normalization of wave function are almost conserved during the numerical calculations. The total system length consisting of the subspace and the lead in our numerical calculations is chosen as $L = \mathcal{N}\delta x = \mathcal{N}l/\mathcal{N}_0$ with the total site number $\mathcal{N}$ (so that the site number of the lead is given by $\mathcal{N} - \mathcal{N}_0$), and we calculate the particle escape dynamics in a time interval in which return of particles to the

subspace from the lead region is negligible. Concrete values of the parameters $\mathcal{N}_0$, $\mathcal{N}$, and $\delta t$ are reported for each numerical result in this paper.

## III. ESCAPE OF ONE FREE PARTICLE

We first consider the case of a single free particle in a semi-infinite one-dimensional space, whose Hamiltonian is given by $\hat{H} = -[\hbar^2/(2m)]\partial^2/\partial x^2$, with the particle position $x \equiv x_1$. Using this Hamiltonian we solve the Schrödinger equation $i\hbar\partial\Psi(x,t)/\partial t = \hat{H}\Psi(x,t)$ for the wave function $\Psi(x,t)$ of the system, for $x \geqslant 0$ and $\Psi(0,t) = 0$, and calculate the survival probability, Eq. (3).

In this system, as shown in Appendix B1, we can solve the Schrödinger equation analytically, and the survival probability $P(t)$ is represented asymptotically as

$$P(t) \overset{t\to+\infty}{\sim} \frac{A_1}{t^3}. \tag{4}$$

Here, the constant $A_1$ is given by

$$A_1 \equiv \frac{2}{3\pi}\left(\frac{ml}{\hbar}\right)^3 \left|\int_0^l dx\; x\; \Psi(x,0)\right|^2, \tag{5}$$

with the wave function $\Psi(x,0)$ at the initial time $t = 0$. Equation (4) means that the survival probability $P(t)$ decays in power $\sim t^{-3}$ asymptotically in time, for arbitrary initial conditions of the subspace as far as $A_1 \neq 0$. Power decays of the survival probability for one-particle systems in a one-dimensional space have been discussed in some papers [6,25,27].

Figure 2 shows graphs of the survival probabilities $P_n(t)$, $n = 1,2,3$ obtained by solving the Schrödinger equation for one free particle numerically, using the subspace site number $\mathcal{N}_0 = 60$, total space site number $\mathcal{N} = 32\,768$, and discretized time interval $\delta t = 10^{-2}$. The energy values corresponding to

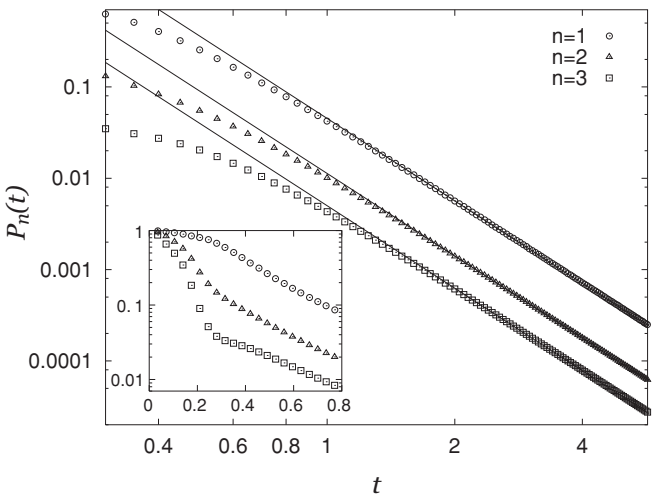


FIG. 2. Survival probabilities $P_n(t), n = 1,2,3$ of one free particle in a semi-infinite one-dimensional space as a function of time $t$ (log-log plots for long-time behavior; inset, linear-log plots for short-time behavior), corresponding to the energies $E_1$ (circles), $E_2$ (triangles), and $E_3$ (squares), respectively. Lines are plots of Eq. (4) with the coefficient, Eq. (5), for the energies $E_n$, $n = 1,2,3$, which are proportional to $t^{-3}$.

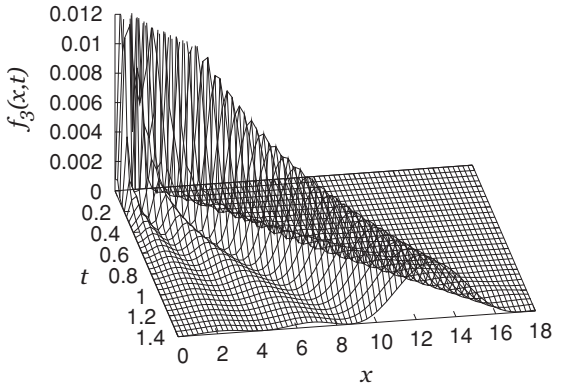


FIG. 3. Probability distribution function $f_3(x,t) \equiv |\Psi_3(x,t)|^2$ of the particle position as a function of $t$ and $x$, corresponding to the energy $E_3$, for one free particle in a semi-infinite one-dimensional space $x \geqslant 0$.

these graphs are $E_1 = 4.77$, $E_2 = 19.1$, and $E_3 = 42.9$. For a comparison, in Fig. 2 we also draw a graph of Eq. (4) with coefficient (5) for each energy. The numerical results for survival probabilities $P_n(t)$, $n = 1,2,3$ in Fig. 2 show a behavior of the power decay $\sim t^{-3}$ independent of $n$ in a large time region, and they agree with our analytical result, Eq. (4), including the value of the coefficient, Eq. (5).

To visualize an escape behavior of one-free-particle systems, in Fig. 3 we show the probability distribution function $f_n(x,t) \equiv |\Psi_n(x,t)|^2$ for $n = 3$ as a function of time $t$ and position $x$. Here, we took the case of $n = 3$ in Fig. 3 so that this spatial distribution $f_3(x,t)$ has three peaks at the initial time $t = 0$, but two of these three peaks decay quickly in time and only one peak survives for a long time and moves away from the subspace region $[0, l]$.

## IV. ESCAPE OF TWO IDENTICAL FREE PARTICLES

As a many-particle effect in escape phenomena, we first discuss the quantum effect of identity of two particles, such as the Pauli exclusion principle, in a semi-infinite one-dimensional system. The Hamiltonian operator of the system is given by $\hat{H} = -[\hbar^2/(2m)](\partial^2/\partial x_1^2 + \partial^2/\partial x_2^2)$, with the position $x_j$ of the $j$th particle ($j = 1,2$), and we impose condition (2) for the wave function $\Psi(x_1,x_2,t)$ as

$$\Psi(x_1,x_2,t) = \pm\Psi(x_2,x_1,t). \tag{6}$$

Here, the plus sign (minus sign) on the right-hand side of Eq. (6) is taken when the particles are identical bosons (fermions). Condition (6) is guaranteed at any time $t$ as far as it is imposed at initial time $t = 0$ because the Hamiltonian operator $\hat{H}$ is invariant under the exchange of the positions of the two particles.

### A. Boson case

In the case of two identical free bosons, as reported in Appendix B 2 a, the asymptotic behavior of the survival probability $P(t)$ is represented as

$$P(t) \overset{t\to+\infty}{\sim} \frac{A_{2b}}{t^6}. \tag{7}$$

Here, $A_{2b}$ is defined by

$$A_{2b} \equiv \frac{4}{9\pi^2}\left(\frac{ml}{\hbar}\right)^6 \left|\int_0^l dx_1 \int_0^l dx_2\, x_1 x_2 \Psi(x_1,x_2,0)\right|^2, \quad (8)$$

with the initial wave function $\Psi(x_1,x_2,0)$. Therefore, in the case of two identical free bosons, the survival probability $P(t)$ decays asymptotically in power $\sim t^{-6}$, which is simply the square of the result of the one free particle discussed in Sec. III.

### B. Fermion case

In the case of two identical free fermions, as reported in Appendix B 2b, the asymptotic behavior of the survival probability $P(t)$ is represented as

$$P(t) \overset{t\to+\infty}{\sim} \frac{A_{2f}}{t^{10}}, \quad (9)$$

with the constant $A_{2f}$ defined by

$$A_{2f} \equiv \frac{2}{4725\pi^2}\left(\frac{ml}{\hbar}\right)^{10} \times \left|\int_0^l dx_1 \int_0^l dx_2\, x_1 x_2 \left(x_1^2 - x_2^2\right)\Psi(x_1,x_2,0)\right|^2. \quad (10)$$

It is important to note that in the case of two identical free fermions, the survival probability $P(t)$ asymptotically decays in the power $\sim t^{-10}$, which is different from the power $\sim t^{-6}$ in the corresponding boson case shown in Eq. (7). In the two identical free fermions the power decay term $\sim t^{-6}$ of the survival probability disappears by a cancellation due to the Pauli exclusion principle $\Phi(x_1,x_2,t) + \Phi(x_2,x_1,t) = 0$, and such fermions escape more rapidly qualitatively than the corresponding two identical free bosons. Effects of Bose or Fermi statistics in quantum escapes in Tonk-Girardeau gases have been discussed in Ref. [26].

## V. ESCAPE OF TWO PARTICLES WITH COULOMB INTERACTIONS

Now we discuss escapes of two particles with Coulomb interactions in a semi-infinite-one-dimensional space. The Hamiltonian operator of the system is given by $\hat{H} = -[\hbar^2/(2m)](\partial^2/\partial x_1^2 + \partial^2/\partial x_2^2) + U(x_1,x_2)$, with the Coulomb potential

$$U(x_1,x_2) = \frac{\lambda}{\sqrt{d^2 + (x_1 - x_2)^2}}. \quad (11)$$

Here, $\lambda$ is a constant representing the strength of Coulomb interactions, and $d$ is a small but nonzero constant introduced as an effect of the quasi-one-dimensionality of the system [35]. Using this Hamiltonian we solve the Schrödinger equation $i\hbar\partial\Psi(x_1,x_2,t)/\partial t = \hat{H}\Psi(x_1,x_2,t)$ for the wave function $\Psi(x_1,x_2,t)$ of this system with condition (6), then calculate the survival probability, Eq. (3).

In this section, we report only results of the two-identical-fermion case, since many results for the corresponding two-identical-boson case are similar to those for the fermion case, except in the limit of weak interactions, where different power decays of survival probabilities between fermions and bosons occur as reported in Sec. IV. Moreover, we discuss effects of Coulomb interactions separately in the two cases: attractive Coulomb interactions and repulsive Coulomb interactions. The repulsive Coulomb interactions corresponding to a positive constant $\lambda$ can be regarded, for example, as those for two electrons, and the attractive interactions corresponding to a negative constant $\lambda$ can be regarded as those for gravitational interactions or, possibly, in an approximated description of systems consisting of an electron and a hole. In this paper we do not take into account collision-like particle-particle interactions even in the case of attractive Coulomb interactions, but the Pauli exclusion principle for identical fermions excludes the possibility of two particles overlapping in space.

### A. Attractive interaction case

First, we consider escapes of two particles with attractive Coulomb interactions with $\lambda < 0$. Figure 4 shows graphs for the survival probabilities $P_n(t)$, $n = 1,2,3,10,15$ as a function of time $t$ for two identical fermions with attractive Coulomb interactions in a semi-infinite one-dimensional space. Here, we used the parameter values $\lambda = -20$ and $d = 10^{-5}$ for potential (11), and also the subspace site number $\mathcal{N}_0 = 20$, the total one-dimensional space site number $\mathcal{N} = 2048$ (so the total site number in two-dimensional $x_1x_2$ space is $\mathcal{N}^2 = 4\,194\,304$), and the discretized time interval $\delta t = 1.5 \times 10^{-3}$. Energy values corresponding to survival probabilities $P_n(t)$, $n = 1,2,3,10,15$ in Fig. 4 are given by $E_1 = -91.0$, $E_2 = -81.1$, $E_3 = -65.7$, $E_{10} = 37.7$, and $E_{15} = 100$, respectively. In Fig. 4 we also show fitting lines for the survival probabilities $P_n(t)$, $n = 1,3,15$, in a large time region to a power decay function $\mu t^{-\nu}$ with fitting parameters $\mu$ and $\nu$. Here, the values of fitting parameters are chosen as $(\mu,\nu) = (8.91 \times 10^{-2}, 2.95)$ for $P_1(t)$, $(\mu,\nu) = (1.09 \times 10^{-2}, 2.85)$ for

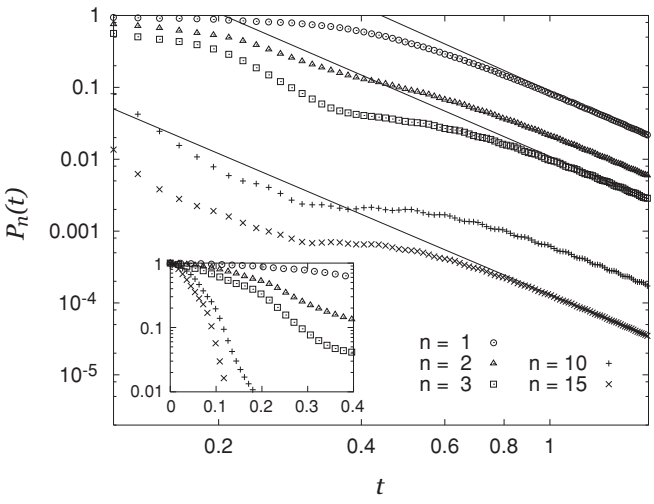


FIG. 4. Survival probabilities $P_n(t)$, $n = 1,2,3,10,15$ for two particles with attractive Coulomb interactions in a semi-infinite one-dimensional space as a function of time $t$ (log-log plots), corresponding to the energies $E_1$ (circles), $E_2$ (triangles), $E_3$ (squares), $E_{10}$ (plus signs), and $E_{15}$ (crosses), respectively. Inset: Linear-log plots of $P_n(t)$ for these energies in a short-time region. Lines are fits for the graphs of $P_n(t)$, $n = 1,3,15$, to a power function $\mu t^{-\nu}$ with fitting parameters $\mu$ and $\nu$.

$P_3(t)$, and $(\mu,\nu) = (1.31 \times 10^{-4}, 2.80)$ for $P_{15}(t)$. These fitting results suggest that after a long time the survival probability $P(t)$ decays in power $\sim t^{-3}$, as in the case of one free particle discussed in Sec. III. This feature could be explained by the fact that two particles with attractive Coulomb interactions behave like one single molecule, so their escape behavior could be similar to that in one-particle cases.

To discuss the molecule-like behavior of two particles with attractive Coulomb interactions, we consider the one-particle spatial distribution function $f_n(x,t)$ defined by

$$f_n(x,t) \equiv \int_0^{+\infty} dx_2\, |\Psi_n(x,x_2,t)|^2 = \int_0^{+\infty} dx_1\, |\Psi_n(x_1,x,t)|^2, \tag{12}$$

noting the relation $|\Psi_n(x_1,x_2,t)|^2 = |\Psi_n(x_2,x_1,t)|^2$ for two identical particles, to derive the second equation in Eq. (12). Figure 5(a) is the graph of the one-particle spatial distribution function $f_n(x,t)$ for $n = 3$ as a function of time $t \in [0,2.03]$ and position $x$. [Here, to calculate the data used in Fig. 5(a), as well as in Fig. 5(b) explained later, we use the same parameter values as in Fig. 4.] As in the one-free-particle case, after some time the one-particle spatial distribution shows one big peak, while the other peaks existing at the initial time decay very rapidly. This one big peak of the one-particle spatial distribution should be due to a one-molecular-like behavior of two particles with attractive Coulomb interactions. Furthermore, we can consider a contribution of each particle in the spatial distribution $f_n(x,t)$ by using the distributions $f_n^{(R)}(x,t)$ and $f_n^{(L)}(x,t)$, defined by

$$f_n^{(R)}(x,t) \equiv \int_x^{+\infty} dx_2 |\Psi_n(x,x_2,t)|^2 = \int_x^{+\infty} dx_1 |\Psi_n(x_1,x,t)|^2, \tag{13}$$

$$f_n^{(L)}(x,t) \equiv \int_0^{x} dx_2 |\Psi_n(x,x_2,t)|^2 = \int_0^{x} dx_1 |\Psi_n(x_1,x,t)|^2. \tag{14}$$

By these definitions, the function $f_n^{(R)}(x,t)$ [$f_n^{(L)}(x,t)$] is the part of $f_n(x,t)$ by the particle with the position whose $x$ value is larger (smaller) than that of the other particle, satisfying the relation

$$f_n(x,t) = f_n^{(R)}(x,t) + f_n^{(L)}(x,t). \tag{15}$$

In this sense, we may regard the distribution $f_n^{(R)}(x,t)[f_n^{(L)}(x,t)]$ as the right-particle component (left-particle component) of the particle spatial distribution $f_n(x,t)$ in a one-dimensional space [36]. Figure 5(b) shows the distributions $f_n^{(R)}(x,t)$ and $f_n^{(L)}(x,t)$ for $n = 3$ at end time $t = 2.03$ shown in Fig. 5(a). The figure shows that the distributions $f_n^{(R)}(x,t)$ and $f_n^{(L)}(x,t)$ are rather overlapped, and both the "right" and the "left" particles contribute to the one big peak in Fig. 5(a) at time $t = 2.03$, implying that two particles are moving together like a single molecule at this time. This feature is very different from the case of repulsive Coulomb interactions, as shown in Sec. V B.

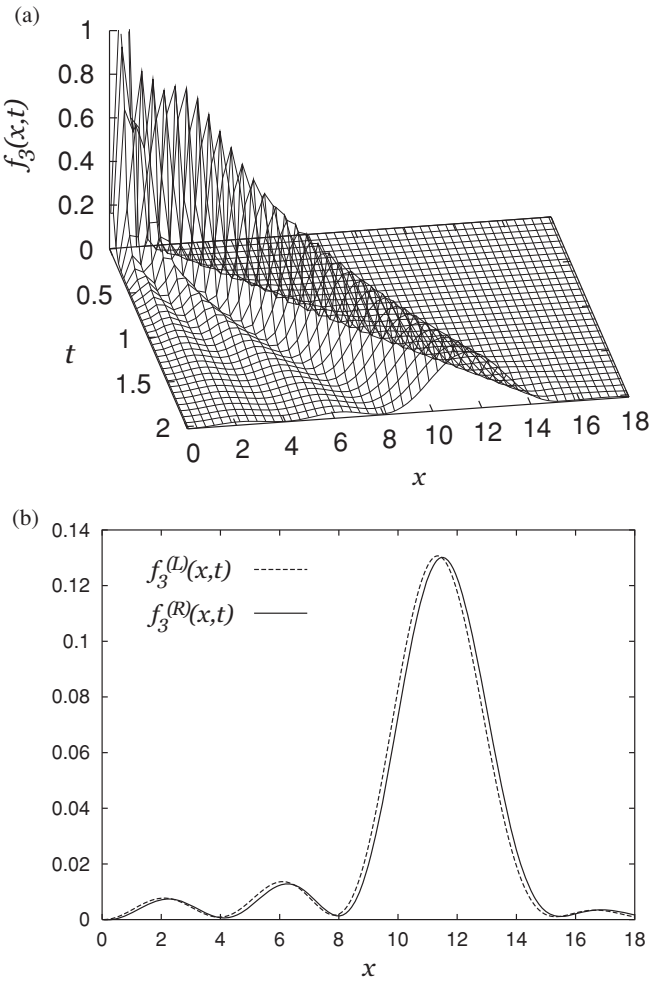


FIG. 5. (a) One-particle spatial distribution function $f_3(x,t) \equiv \int_0^{+\infty} dx_2\, |\Psi_3(x,x_2,t)|^2$ as a function of time $t \in [0,2.03]$ and position $x$, corresponding to the energy $E_3$, for two particles with attractive Coulomb interactions in a semi-infinite one-dimensional space $x \geqslant 0$. (b) Right-particle component of the spatial distribution $f_3^{(R)}(x,t) \equiv \int_x^{+\infty} dx_2\, |\Psi_3(x,x_2,t)|^2$ and left-particle component of spatial distribution $f_3^{(L)}(x,t) \equiv \int_0^{x} dx_2\, |\Psi_3(x,x_2,t)|^2$ as a function of position $x$ at time $t = 2.03$.

It is also important to note in Fig. 4 that the survival probability $P(t)$ decays in power $\sim t^{-3}$ even in high-energy cases. In high-energy cases of $E_n > 0$, the average energy is higher than the value of the attractive potential energy [which is negative by Eq. (11) with $\lambda < 0$] and can have enough energy to break a binding force of two particles by attractive interactions in a classical mechanical sense. However, even in the cases of $E_{10} = 37.7$ and $E_{15} = 100$ in Fig. 4, the survival probabilities still decay in power $\sim t^{-3}$ after a long time, as in the one-free-particle case. A possible way to explain this behavior is that in the open systems considered here, each escape state of a two-particle system is expressed as a superposition of energy eigenstates of the open system, and (because particles with a higher energy would escape more quickly) main contributions to the survival probability after a long time would come from those with low energies in which two particles have to behave like a molecule, leading to the

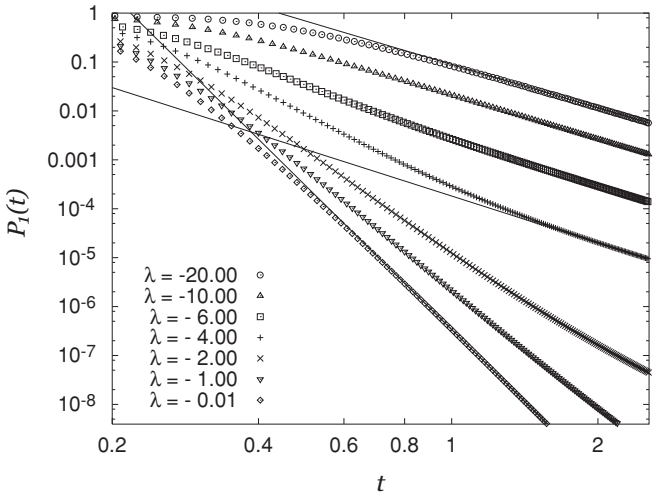


FIG. 6. Survival probability $P_1(t)$ for two particles with attractive Coulomb interactions corresponding to the energy $E_1$ in a semi-infinite one-dimensional space as a function of time $t$ (log-log plots), for the interaction strengths $\lambda = -20$ (circles), $\lambda = -10$ (triangles), $\lambda = -6$ (squares), $\lambda = -4$ (plus signs), $\lambda = -2$ (crosses), $\lambda = -1$ (inverted triangles), and $\lambda = -0.01$ (diamonds). Lines are fits for the graphs of $P_1(t)$ for $\lambda = -20, -4, -0.01$ to a power function $\mu t^{-\nu}$ with fitting parameters $\mu$ and $\nu$.

power decay $\sim t^{-3}$ as in the one-particle case, even though the average energy $E_n$ of the system could be very high.

Although the survival probability decays in power $\sim t^{-3}$ in Fig. 4 as in the one-free-particle case, it should decay in a different power, $\sim t^{-10}$, in the weak interaction limit $\lambda \to 0$, consistent with the results for two identical free fermions. To discuss such a transition from the power decay $\sim t^{-3}$ to the other power decay $\sim t^{-10}$ as the absolute value $|\lambda|$ of interaction strength decreases, we show in Fig. 6 graphs of the survival probabilities $P_1(t)$ for two particles with attractive Coulomb interactions as a function of time $t$ for different interaction strengths: $\lambda = -20, -10, -6, -4, -2, -1$, and $-0.01$. Here, we used the same parameter values as in Fig. 4, except for the values of $\lambda$, for $N = 4096$ in the cases of $\lambda = -2, -1$ and for $\delta t = 4 \times 10^{-3}$ in the cases of $\lambda = -2, -1, -0.01$. The values of $E_1$ corresponding to the cases shown in Fig. 6 are $-91.0$, $-18.4$, 0.741, 8.69, 15.8, 19.1, and 22.2 for $\lambda = -20, -10, -6, -4, -2, -1$, and $-0.01$, respectively. Figure 6 shows that the time region of the power decay $\sim t^{-3}$ of the survival probability becomes later as the absolute value $|\lambda|$ of the interaction strength decreases from $|\lambda| = 20$ (see the cases of $\lambda = -20, -10, -6$, and $-4$ in Fig. 6), and a more rapid decay behavior closer to $t^{-10}$ appears as the value of $|\lambda|$ becomes very small (see the case of $\lambda = -0.01$ in Fig. 6). To clarify these behaviors quantitatively we also fitted the survival probabilities for $\lambda = -20, -4$, and $-0.01$ to a power function $\mu t^{-\nu}$ with fitting parameter values $(\mu, \nu) = (8.91 \times 10^{-2}, 2.95)$ for $\lambda = -20$, $(\mu, \nu) = (1.82 \times 10^{-4}, 3.17)$ for $\lambda = -4$, and $(\mu, \nu) = (3.36 \times 10^{-7}, 9.79)$ for $\lambda = -0.01$ in Fig. 6. Comparison of these fitting lines with the corresponding survival probabilities shows that in the case of $\lambda = -20$, the survival probability $P_1(t)$ decays almost in power $\sim t^{-3}$ after about the time $t = \tilde{\tau} \approx 1.4$, while in the case of $\lambda = -4$ it decays almost in the same power after about time $t \approx 1.8$, later than time $t = \tilde{\tau}$. On the other hand, in the case of $\lambda = -0.01$ the power decay $\sim t^{-10}$ is a good approximation of the survival probability $P_1(t)$ after about time $t \approx 0.8$. This feature of $\lambda$ dependence in the decay of the survival probability could be explained by the fact that, in an escape state expressed as a superposition of various energy eigenstates of the open system, the long-time behavior of particles in the subspace is dominated by the molecular-like behavior of two-particle states with a very low energy, causing the power decay $\sim t^{-3}$ in a very-long-time region even in a weak interaction case, although for the cases of very weak interactions a behavior similar to that for two-free-particle cases appears in some time regions.

### B. Repulsive interaction case

Now we consider escapes of two particles with repulsive Coulomb interactions with $\lambda > 0$. Figure 7 shows graphs for the survival probabilities $P_n(t)$, $n = 1,2,3,9,16,19$ as a function of time $t$ for two identical fermions with repulsive Coulomb interactions in a semi-infinite one-dimensional space. Here, we used the parameter values $\lambda = 50$ and $d = 10^{-5}$ for potential (11), and also the subspace site number $\mathcal{N}_0 = 60$, the total one-dimensional space site number $\mathcal{N} = 2048$, and the discretized time interval $\delta t = 10^{-3}$ for $n = 1,2,3,9,16$ and $\delta t = 8 \times 10^{-4}$ for $n = 19$. Energy values corresponding to the survival probabilities $P_n(t)$, $n = 1,2,3,9,16,19$ in Fig. 7 are given by $E_1 = 131$, $E_2 = 181$, $E_3 = 192$, $E_9 = 330$, $E_{16} = 455$, and $E_{19} = 507$, respectively. Repulsive interactions have the effect of making particles farther apart from each other in distance and lead to faster decay of the survival probability $P_n(t)$ than in the case for free or attractively interacting particles. Actually,

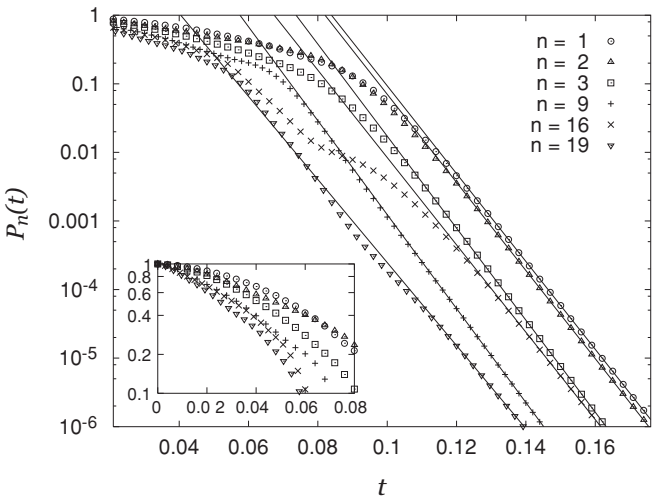


FIG. 7. Survival probabilities $P_n(t)$, $n = 1,2,3,9,16,19$ for two particles with repulsive Coulomb interactions in a semi-infinite one-dimensional space as a function of time $t$ (linear-log plots), corresponding to the energies $E_1$ (circles), $E_2$ (triangles), $E_3$ (squares), $E_9$ (plus signs), $E_{16}$ (crosses), and $E_{19}$ (inverted triangles), respectively. Inset: Linear-log plots of $P_n(t)$ for these energy cases in a short-time region. Lines are fits for the survival probabilities $P_n(t)$, $n = 1,2,3,9,16,19$ to an exponential function $\mathcal{A} \exp(-\alpha t)$ with fitting parameters $\mathcal{A}$ and $\alpha$.

Fig. 7 shows that decay of the survival probability $P_n(t)$ for repulsively Coulomb-interacting two particles is well approximated as an exponential decay after a short time, which is much faster than power decays in the cases of one free particle, two free particles, and two attractively Coulomb-interacting particles discussed in Secs. III, IV, and V A. In Fig. 7 we also show a fitting line for each survival probability $P_n(t)$ to an exponential function $\mathcal{A}\exp(-\alpha t)$ with the fitting parameter $\mathcal{A}$ and $\alpha$. Here, the values of fitting parameters are chosen as $(\mathcal{A},\alpha) = (2.37 \times 10^5, 147)$ for $P_1(t)$, $(\mathcal{A},\alpha) = (1.87 \times 10^5, 148)$ for $P_2(t)$, $(\mathcal{A},\alpha) = (8.83 \times 10^4, 154)$ for $P_3(t)$, $(\mathcal{A},\alpha) = (8.73 \times 10^3, 158)$ for $P_9(t)$, $(\mathcal{A},\alpha) = (1.97 \times 10^4, 147)$ for $P_{16}(t)$, and $(\mathcal{A},\alpha) = (2.81 \times 10^2, 139)$ for $P_{19}(t)$. The escape rate, defined by the parameter $\alpha$, does not depend strongly on the value of the energy $E_n$ in these numerical results. This feature of the escape rate of the survival probability could be explained by a feature of the escape state represented as a superposition of various energy eigenstates of the open system. Since the escape state includes various energy states and the main contribution to the survival probability could come from low-energy states after a long time, the decay rate $\alpha$ of the survival probability determined by low-energy states could be independent of the average energy $E_n$ of particles.

As a general tendency, particles with a higher energy $E_n$ escape faster, with a lower value of the survival probability, but this is not always true. The graphs in Fig. 7 include an example of a higher survival probability $P_n(t)$ for a higher energy $E_n$; concretely speaking, $P_9(t) < P_{16}(t)$ for $E_9 < E_{16}$ after a time $\tilde{t} \approx 0.09$, although $P_{16}(t) < P_9(t)$ for a short-time region. This kind of behavior of survival probabilities, that is, $P_n(t) < P_{n'}(t)$ for $E_n < E_{n'}$ at some times, is sometimes observed in two-particle systems with Coulomb interactions.

Figure 8(a) is a graph of the one-particle spatial distribution function $f_n(x,t)$ defined by Eq. (12) for $n = 3$ as a function of time $t$ and position $x$. This figure clearly shows that two peaks corresponding to two particles can survive for a long time, although there are many peaks in a short-time region. The position of one of these two peaks closer to the wall at $x = 0$ does not change very much in time, probably because the particle corresponding to this peak receives a repulsive Coulomb force from another particle in the direction of the wall and its escape movement is suppressed. On the other hand, the position of another peak moves away quickly from the subspace. This interpretation of these two peaks as behaviors of different particles in the one-particle spatial distribution function $f_n(x,t)$ could be justified by the right-particle component of spatial distribution (13) and the left-particle component of spatial distribution (14), which are shown in Fig. 8(b) at time $t = 0.172$, that is, at the final time shown in Fig. 8(a). Figure 8(b) suggests that at time $t = 0.172$ the right-hand peak of $f_3(x,t)$ consists of the right particle represented by a peak of the distribution $f_3^{(R)}(x,t)$, and the left-hand peak of $f_3(x,t)$ consists of the left particle represented by a peak of the distribution $f_3^{(L)}(x,t)$. It should be noted that, differently from Fig. 5(d) for two particles with attractive Coulomb interactions, the peaks of distributions (13) and (14) are clearly separated for two particles with repulsive Coulomb interactions in Fig. 8(b).

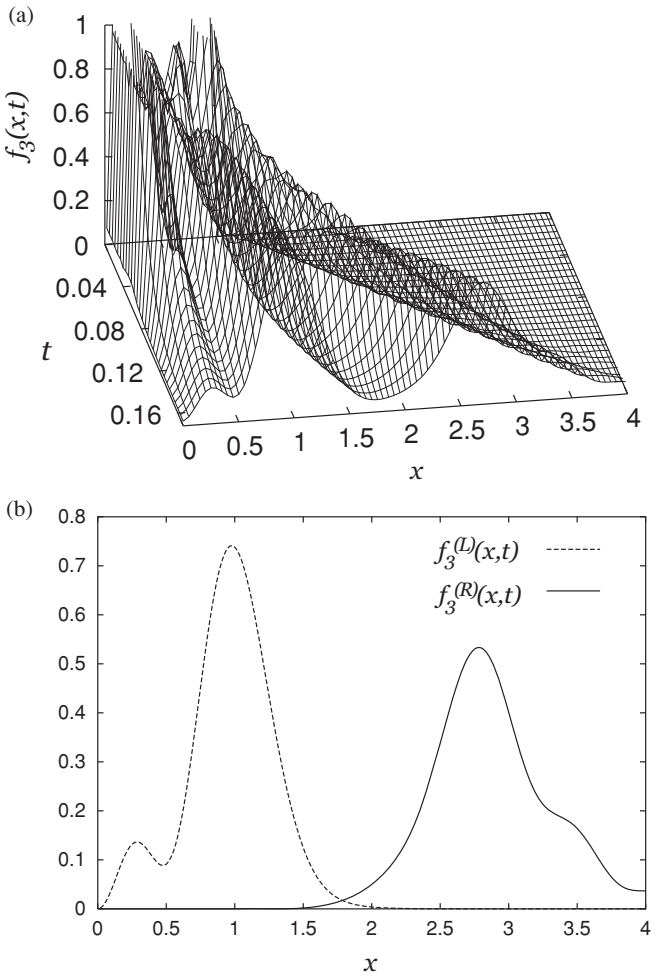


FIG. 8. (a) One-particle spatial distribution function $f_3(x,t) \equiv \int_0^{+\infty} dx_2\, |\Psi_3(x,x_2,t)|^2$ as a function of time $t \in [0,0.172]$ and position $x$, corresponding to the energy $E_3$, for two particles with repulsive Coulomb interactions in a semi-infinite one-dimensional space $x \geqslant 0$. (b) Right-particle component of spatial distribution $f_3^{(R)}(x,t) \equiv \int_x^{+\infty} dx_2\, |\Psi_3(x,x_2,t)|^2$ and left-particle component of spatial distribution $f_3^{(L)}(x,t) \equiv \int_0^{x} dx_2\, |\Psi_3(x,x_2,t)|^2$ as a function of position $x$ at time $t = 0.172$.

Now, we discuss an interaction strength $\lambda$ dependence of the survival probability $P_n(t)$. In Fig. 9 we plot the survival probability $P_1(t)$ as a function of time $t$ for $\lambda = 50,20,5,0.5,0.001$. Here, we used the parameter values $\mathcal{N}_0 = 60$, $d = 10^{-5}$, and also $\delta t = 10^{-3}$ for $\lambda = 50,20,5$, $\delta t = 5 \times 10^{-3}$ for $\lambda = 0.5,0.001$, $\mathcal{N} = 2048$ for $\lambda = 50$, and $\mathcal{N} = 4096$ for $\lambda = 20,5,0.5,0.001$. The values of $E_1$ for the cases shown in Fig. 9 are 131, 73.7, 38.5, 25.4, and 23.9 for $\lambda = 50$, 20, 5, 0.5, and 0.001, respectively. This figure shows that in the case of very weak interactions such as $\lambda = 0.001$, the survival probability decays in power rather close to $t^{-10}$ as in the two-free-fermion case. To clarify this point, in Fig. 9 we fit the survival probability $P_1(t)$ for $\lambda = 0.001$ to the function $\mu t^{-\nu}$ with fitting parameter values $(\mu,\nu) = (2.25 \times 10^{-7}, 9.49)$. In other words, a transition from an exponential decay to a power decay occurs in the survival probability of two particles with repulsive Coulomb interactions in a semi-infinite

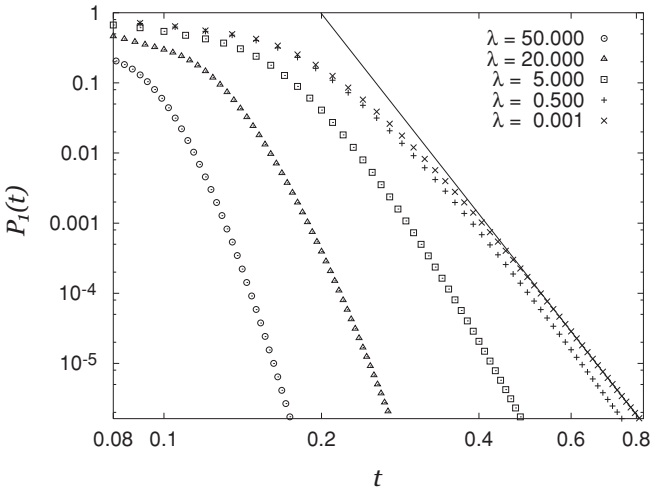


FIG. 9. Survival probability $P_1(t)$ for two particles with repulsive Coulomb interactions corresponding to the energy $E_1$ in a semi-infinite one-dimensional space as a function of time $t$ (log-log plots), for the interaction strengths $\lambda = 50$ (circles), $\lambda = 20$ (triangles), $\lambda = 5$ (squares), $\lambda = 0.5$ (plus signs), and $\lambda = 0.001$ (crosses). Lines are a fit for the graph of $P_1(t)$ for $\lambda = 0.001$ to a power function $\mu t^{-\nu}$ with fitting parameters $\mu$ and $\nu$.

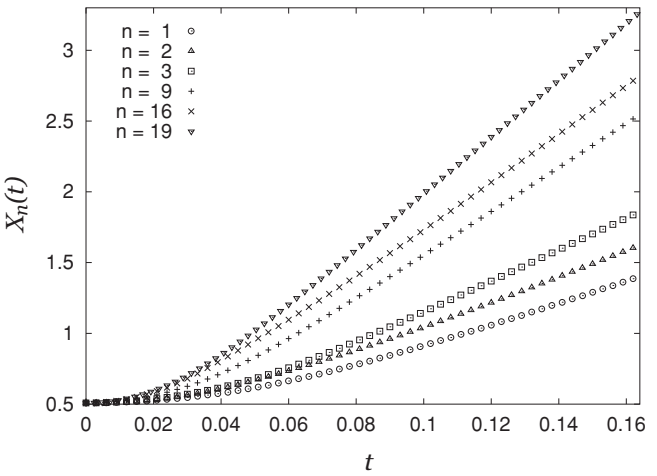


FIG. 10. Average particle position $X_n(t) \equiv \int_0^{+\infty} dx_1 \int_0^{+\infty} dx_2\, x_1 |\Psi_n(x_1,x_2,t)|^2$, $n = 1,2,3,9,16,19$ for two-fermion systems with repulsive Coulomb interactions in a semi-infinite one-dimensional space as a function of time $t$ (linear-linear plots), corresponding to the energies $E_1$ (circles), $E_2$ (triangles), $E_3$ (squares), $E_9$ (plus signs), $E_{16}$ (crosses), and $E_{19}$ (inverted triangles), respectively.

one-dimensional system, as the value of the interaction strength $\lambda(\geqslant 0)$ decreases.

So far, we have considered mainly properties of the subspace via the survival probability of escapes in a semi-infinite one-dimensional space, but escape phenomena can also be regarded as a driving source to produce a particle current. From this point of view, we consider the average position

$$X_n(t) \equiv \int_0^{+\infty} dx_1 \int_0^{+\infty} dx_2\, x_1 |\Psi_n(x_1,x_2,t)|^2 \qquad (16)$$

of a particle in whole space at time $t$, corresponding to the energy $E_n$. Differently from the survival probability, which is determined by information on two particles within the subspace $[0,l]$ only, this average position $X_n(t)$ is determined by information on the particles in all space $[0,+\infty)$, and its time dependence can be an indicator of particle currents produced by the escape dynamics. Figure 10 shows graphs of $X_n(t)$ as a function of time $t$ for $n = 1,2,3,9,16,19$, where we used the same parameter values as used to obtain the results shown in Fig. 7, and the time interval in Fig. 10 is also almost the same as in Fig. 7. Figure 10 shows that each particle moves with a stable constant average velocity, as indicated by a constant slope of $X_n(t)$ as a function of $t$, after a short time. It is important to note that, roughly speaking, this constant-velocity movement of the average particle position seems to occur when an exponential decay of the survival probability in Fig. 7 appears. One should also notice that in all cases shown in Fig. 10 a particle with a higher energy $E_n$ moves faster on average, even for $n = 9,16$ satisfying the inequality $X_9(t) < X_{16}(t)$, although the corresponding survival probability with higher energy $E_n$ does not always take a smaller value after a long time, for example, $P_9(t) < P_{16}(t)$ for $t > \tilde{t} \approx 0.09$, as shown in Fig. 7. A constant slope in the average position $X_n(t)$ as a function of $t$ appears not only in two-particle systems with repulsive Coulomb interactions, but also in other systems such as one free particle, two free particles, and two attractively Coulomb-interacting particles, although we do not show graphs of $X_n(t)$ for those cases in this paper.

## VI. CONCLUSION AND REMARKS

In this paper we have discussed quantum escape behaviors of one- and two-particle systems with and without Coulomb interactions from a one-dimensional finite subspace to a semi-infinite one-dimensional lead. For these particle escapes, we prepared the wave function of the system at initial time $t = 0$ as an energy eigenstate of particles confined within the subspace, and we calculated the survival probability for all particles to stay within the subspace at time $t$. We showed analytically that the survival probability decays in power $\sim t^{-3}$ asymptotically for one free particle, and it decays in power $\sim t^{-10}$ ($\sim t^{-6}$) for two identical free fermions (bosons) upon taking into account quantum effects of two identical particles, such as the Pauli exclusion principle. On the other hand, it is shown numerically that two identical fermions with attractive Coulomb interactions behave like one single molecule, so their survival probability decays in power $\sim t^{-3}$ after a long time, as in the one-free-particle case. Moreover, we showed numerically that for two identical fermions with repulsive Coulomb interactions, the survival probability decays exponentially $\sim \exp(-\alpha t)$ in time. Our results suggest that the decay rate $\alpha$ of the survival probability in the cases of repulsive Coulomb interactions is almost independent of the initial particle energy.

Although we showed an exponential decay of the survival probability for two particles with repulsive Coulomb particle-particle interactions, it is meaningful to note that an exponential decay of the survival probability could occur even in one-particle systems. As such an example, in Fig. 11 we show the survival probabilities $P_n(t)$, $n = 1,2,3$ for the one-particle system with a very localized single potential

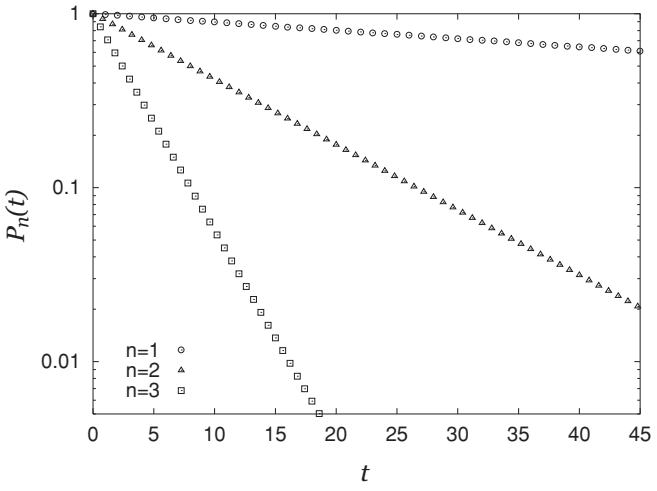


FIG. 11. Survival probabilities $P_n(t)$, $n = 1,2,3$ of a one-particle system with a localized single potential barrier in a semi-infinite one-dimensional space as a function of time $t$ (linear-log plots), corresponding to the particle energies $E_1$ (circles), $E_2$ (triangles), and $E_3$ (squares), respectively. Here, the potential barrier is located just outside the subspace, and the potential magnitude of the barrier is chosen to be very strong in comparison with the particle energies.

barrier at a site just outside the subspace in a semi-infinite one-dimensional space, where we used parameter values as the subspace site number $\mathcal{N}_0 = 60$, the total space site number $\mathcal{N} = 32\,768$, and the discretized time interval $\delta t = 2 \times 10^{-4}$. Here, we chose the potential magnitude of the single site barrier as $1.8 \times 10^3$, which is much larger than the particle energies $E_1 = 4.77$, $E_2 = 19.1$, and $E_3 = 42.9$. Figure 11 shows a clear exponential decay of the survival probability for such a one-particle system with a strong potential barrier [26,27]. However, in Fig. 11 the exponential decay rates of the survival probabilities for this one-particle case with a potential barrier depend strongly on the value of their particle energies, different from the results for two-particle systems with repulsive Coulomb-interactions shown in Fig. 7. This energy-dependent exponential decay rates can be explained by the fact that particle escape via a strong potential barrier is caused by quantum tunneling, and such quantum tunneling can occur more strongly for a particle with a higher energy.

An interesting problem in escape phenomena is their quantum-classical correspondence. This is a nontrivial problem even in a very simple system such as a one-free-particle system, because the survival probability of nonchaotic classical systems is generally supposed to decay in power $t^{-1}$ [16], while the survival probability of a free particle in a semi-infinite one-dimensional space decays in a different power $\sim t^{-3}$ as shown in this paper. As a first attempt to discuss classical mechanical escapes corresponding to the quantum escapes discussed in this paper, we consider classical mechanical two-particle systems with Coulomb interactions in a semi-infinite one-dimensional space. We define the classical survival probability $P(t)$ for classical mechanical two-particles as the probability of both the particles

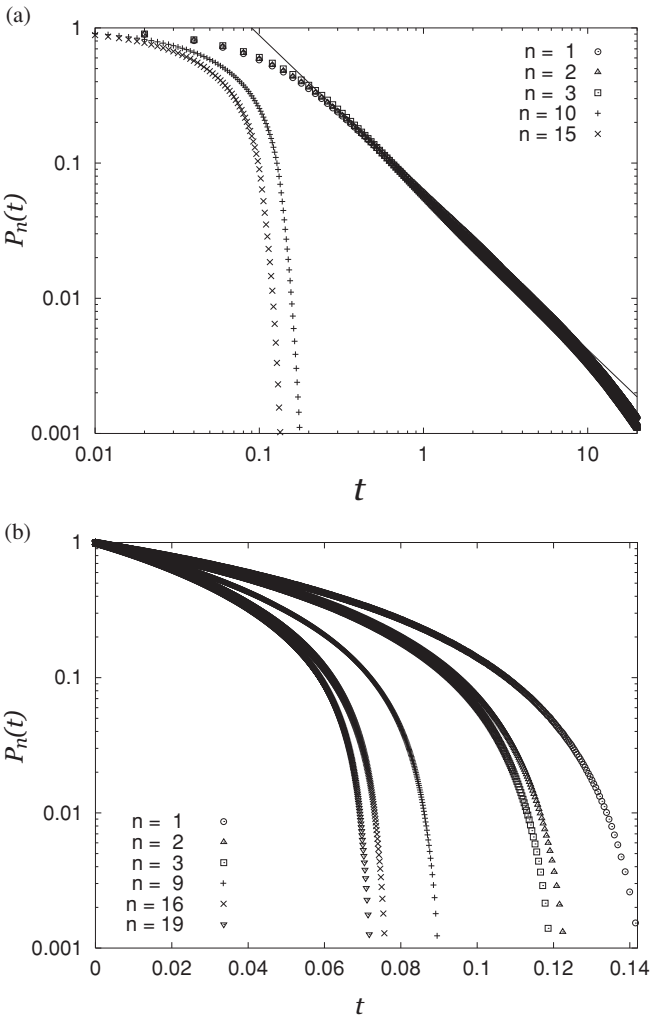


FIG. 12. (a) Classical survival probabilities $P_n(t)$, for $n = 1$ (circles), $n = 2$ (triangles), $n = 3$ (squares), $n = 10$ (plus signs), and $n = 15$ (crosses) for two classical mechanical particles with attractive Coulomb interactions in a semi-infinite one-dimensional space as a function of time $t$ (log-log plots). Line is a fit for the graph of $P_1(t)$ to a power function $\mu t^{-\nu}$ with fitting parameters $\mu$ and $\nu$. (b) Classical survival probabilities $P_n(t)$, for $n = 1$ (circles), $n = 2$ (triangles), $n = 3$ (squares), $n = 9$ (plus signs), $n = 16$ (crosses), and $n = 19$ (inverted triangles) for classical mechanical two-particle systems with repulsive Coulomb interactions in a semi-infinite one-dimensional space as a function of time $t$ (linear-log plots).

staying within the subspace at time $t$, and to discuss a quantum-classical correspondence we introduce the probability $P_n(t)$ as the classical survival probability of the system with the initial particle distribution represented as an ensemble of particles with the constant energy $E_n$ whose value is the same as the energy eigenvalue of the initial state in the corresponding quantum system [37]. In Fig. 12(a) we show graphs of such classical survival probabilities $P_n(t)$, $n = 1,2,3,10,15$ for classical mechanical two-particles with attractive Coulomb interactions. Here, we used the same parameter values of $l$, $\lambda$, and $d$, and the same values of $E_n$, $n = 1,2,3,10,15$, as in the corresponding quantum two-particle cases whose quantum survival probabilities are shown in Fig. 4. In this

figure, the survival probabilities $P_n(t), n = 1,2,3$ have quite similar values and it is hard to distinguish them. One may notice a time period for the graphs of $P_n(t), n = 1,2,3$ in which the survival probability seems to decay in power, so we fit the graph of $P_1(t)$ to a power function $\mu t^{-\nu}$ with fitting parameter values $(\mu,\nu) = (6.06 \times 10^{-2}, 1.16)$, close to a power decay $\sim t^{-1}$. However, we cannot recognize such a power decay for $P_n(t), n = 10,15$ in Fig. 12(a). In Fig. 12(b) we also show graphs of such classical survival probabilities $P_n(t)$, $n = 1,2,3,9,16,19$ for classical mechanical two-particles with repulsive Coulomb interactions. Here, we used the same parameter values of $l$, $\lambda$, and $d$, and the same values of $E_n$, $n = 1,2,3,9,16,19$, as in the corresponding quantum two-particle cases whose quantum survival probabilities are shown in Fig. 7. It is shown that in Fig. 12(b) the classical survival probabilities of the systems with repulsive Coulomb interactions do not decay exponentially in time and they rather seem to go to 0 at a finite time. In both cases shown in Figs. 12(a) and 12(b), it is rather hard to discuss a direct quantitative connection of the quantum escapes with the corresponding classical escapes. However, we should notice many problems in comparing Fig. 4 and Fig. 12(a), as well as Fig. 7 and Fig. 12(b), as a quantum-classical correspondence of particle escapes. First, quantum-classical correspondence is generally realized in a high-energy region, and realization of classical states corresponding to quantum low energy states, such as the ground state and the first and second exited states discussed in this paper, would be difficult. As another point of difference from the quantum escapes discussed in this paper, in the classical cases shown in Fig. 12 we chose an ensemble of particles with a fixed energy $E_n$ initially and the system in the escape state always has this fixed energy only, while the quantum escape state discussed in this paper is represented as a superposition of eigenstates of the open system with various energies even if the initial state is chosen as the energy eigenstate of particles confined in the subspace with a fixed energy $E_n$. To solve these problems and to compare quantitatively quantum escapes with the corresponding classical escapes for two-particle systems with Coulomb interactions, as well as more detailed discussions on classical escapes in semi-infinite one-dimensional systems, are important future problems.

One may notice that in this paper, exponential decays of survival probabilities in two-particle systems with repulsive Coulomb interactions are shown numerically, so there is still the possibility that it might be only a finite time property and it might decay in power in the long-time limit $t \to +\infty$. Related to this remark, Refs. [6] and [27] argued that the survival probability of one-particle systems with a $\delta$-functional potential barrier in an effectively semi-infinite one-dimensional space decays in power in the long-time limit, even if it shows an exponential decay for a finite-time region as in Fig. 11. However, it should be valuable to show some results on particle-particle interaction effects in escape behaviors even if they are finite-time properties.

In future it would be interesting to investigate the relation of quantum escapes with chaotic dynamics in two-particle systems with Coulomb interactions. The strength of chaos in quantum systems can be investigated, for example, by using energy level spacing distributions [38–40], and quantum chaos in many-electron systems with Coulomb interactions in a finite region have been discussed for two-particle systems in a one-dimensional space [35], in a one-dimensional space with a random potential [41], and in a two-dimensional space [42,43], as well as for three-particle systems [44]. However, different from closed systems considered in these past papers, the system for particles to escape is an open system in which the energy spectrum is continuous, and analysis of chaos by energy level spacing distributions is not applicable to such an open system. Even in the classical case, analysis of chaos in open systems without a confining potential barrier could be very different from that in closed systems or billiard systems with a small hole, because particles can go very easily to an infinite region without being trapped in a finite region. In this sense, to clarify a relation between the chaotic property of many-particle systems with Coulomb interactions and decay behaviors of the survival probability is highly nontrivial and remains an unsettled problem. It would also be important to investigate escape behaviors of systems consisting of more than two particles, although to study such a large system numerically we would need much better numerical resources and techniques than those used to obtain the results in this paper. Such large systems with particle-particle interactions could be more strongly chaotic than two-particle systems, and they could provide better situations for studying quantum chaotic effects in escape phenomena. We could also consider the particle escape of such a large number of particles as a driving source to produce a particle current from a particle reservoir. For this case, as the initial state we could choose an equilibrium (e.g. canonical) state, which is represented as the density matrix given by the energy eigenstates $\{\Phi_n(x_1,x_2,\ldots,x_N)\}_n$ used in this paper, with the weight of an equilibrium distribution.

## ACKNOWLEDGMENTS

One of the authors (T.T.) is grateful to P. A. Jacquet and C. P. Dettmann for stimulating discussions and useful comments about escape problems. This research was supported by the grant sponsor "Open Research Project for Physical Science of Biomolecular Systems," funded by the Ministry of Education, Culture, Sports, Science, and Technology of Japan.

## APPENDIX A: NUMERICAL CALCULATIONS OF A ONE-DIMENSIONAL TWO-PARTICLE DYNAMICS

In this Appendix we represent how we discretized the Schrödinger equation for a system consisting of two particles in a semi-infinite one-dimensional space to calculate the survival probability $P(t)$ in this paper. Especially, we show a spatially discretized Hamiltonian and outline the pseudospectral method used to solve the Schrödinger equation discretized in time.

### 1. Spatial discretization of the Hamiltonian operator

We consider two particles in a semi-infinite one-dimensional space and take $x_j (\geqslant 0)$ as the position coordinate of the $j$-th particle, $j = 1,2$. Then, we discretize the semi-infinite one-dimensional space by a positive constant $\delta l$, so $x_j \to n_j \delta l$, $n_j = 0,1,2,\ldots$ for $j = 1,2$. In this discretization

of the one-dimensional space, the spatially second derivative $\partial^2/\partial x_j^2$ applying to any function $X(x_j)$ is represented as

$$\frac{\partial^2 X(x_j)}{\partial x_j^2} \to \frac{\tilde{X}(n_j+1)-2\tilde{X}(n_j)+\tilde{X}(n_j-1)}{\delta l^2} \equiv -\frac{1}{\delta l^2}\sum_{k=0}^{+\infty}\mathcal{K}_{n_j k}\tilde{X}(k) \tag{A1}$$

where $\tilde{X}(n_j) \equiv X(n_j\delta l)$ is the spatially discretized function of $X(x_j)$. Here, the matrix $\mathcal{K} \equiv (\mathcal{K}_{jk})$, $j = 0,1,2,\ldots$, $k = 0,1,2,\ldots$, is the matrix whose only nonzero elements are $\mathcal{K}_{jj} = 2$ and $\mathcal{K}_{(j+1)j} = \mathcal{K}_{j(j+1)} = -1$, $j = 0,1,2,\ldots$. Using Eq. (A1), the Hamiltonian operator $\hat{H}$ is represented as the matrix $H$ for the spatially discretized representation:

$$\hat{H} \to H \equiv \frac{\hbar^2}{2m\delta l^2}K + \tilde{U}(\mathbf{n})I \tag{A2}$$

with $\mathbf{n} \equiv (n_1,n_2)$ and $\tilde{U}(\mathbf{n}) \equiv U(n_1\delta l, n_2\delta l)$ using the potential $U(x_1,x_2)$ given by Eq. (11) for the continuous space case. Here, the matrices $K \equiv (K_{\mathbf{nn}'})$ and $I \equiv (I_{\mathbf{nn}'})$ are defined by

$$K_{\mathbf{nn}'} \equiv \mathcal{K}_{n_1n_1'}\delta_{n_2n_2'} + \delta_{n_1n_1'}\mathcal{K}_{n_2n_2'}, \tag{A3}$$

$$I_{\mathbf{nn}'} \equiv \delta_{n_1n_1'}\delta_{n_2n_2'}, \tag{A4}$$

respectively, for any $\mathbf{n} \equiv (n_1,n_2)$ and $\mathbf{n}' \equiv (n_1',n_2')$. Using Eq. (A2) the Schrödinger equation is spatially discretized as $i\hbar\partial\tilde{\boldsymbol{\Psi}}(t)/\partial t = H\tilde{\boldsymbol{\Psi}}(t)$ as a equation for the vector $\tilde{\boldsymbol{\Psi}}(t) \equiv (\tilde{\Phi}(\mathbf{n},t))$ defined by $\tilde{\Phi}(\mathbf{n},t) \equiv \Psi(n_1\delta l, n_2\delta l, t)$ with the vector index $\mathbf{n}$.

It may be meaningful to represent the Hamiltonian matrix $H$ by using the Dirac notation. Introducing a set of the state $|\mathbf{n}\rangle$ as those forming a complete ($\sum_{\mathbf{n}}|\mathbf{n}\rangle\langle\mathbf{n}| = 1$) and orthogonal ($\langle\mathbf{n}|\mathbf{n}'\rangle = \delta_{n_1n_1'}\delta_{n_2n_2'}$) set for the site indexes $\mathbf{n}$ and $\mathbf{n}'$, the Hamiltonian matrix $H$ can be represented as the operator

$$\hat{\mathcal{H}} \equiv \sum_{\mathbf{n}}|\mathbf{n}\rangle\epsilon_{\mathbf{n}}\langle\mathbf{n}| + u\sum_{\substack{\mathbf{n},\mathbf{n}'\\(|\mathbf{n}-\mathbf{n}'|=1)}}|\mathbf{n}\rangle\langle\mathbf{n}'| \tag{A5}$$

where $\epsilon_{\mathbf{n}}$ and $u$ are defined by $\epsilon_{\mathbf{n}} \equiv [2\hbar^2/(m\delta l^2)] + U(n_1\delta l, n_2\delta l)$ and $u \equiv -\hbar^2/(2m\delta l^2)$, respectively. The operator (A5) has the same type of form as a tight-binding Hamiltonian with the site energy $\epsilon_{\mathbf{n}}$ and the hopping rate $u$, and the Schrödinger equation is represented as $i\hbar\partial|\Psi(t)\rangle/\partial t = \hat{\mathcal{H}}|\Psi(t)\rangle$ as a equation for the state $|\Psi(t)\rangle \equiv \sum_{\mathbf{n}}\tilde{\Phi}(\mathbf{n},t)|\mathbf{n}\rangle$.

### 2. Time discretization of the Schrödinger equation by the pseudospectral method

In the previous subsection of this Appendix we discussed how we spatially discretized the Hamiltonian operator. In this subsection we outline how we discretize the time-evolution by the Schrödinger equation in the way called by the pseudo-spectral method.

We consider a one-dimensional space of the length $L$ consisting of the subspace and the lead, and note that the function $\mathcal{X}(x_1,x_2)$ of $x_1$ and $x_2$ satisfying the boundary condition $\mathcal{X}(0,x_2) = \mathcal{X}(x_1,0) = \mathcal{X}(L,x_2) = \mathcal{X}(x_1,L) = 0$ can be Fourier-transformed as

$$\tilde{\mathcal{X}}(k_1,k_2) = \sqrt{\frac{2}{L}}\int_0^L dx_1\int_0^L dx_2\mathcal{X}(x_1,x_2) \times \sin\left(\frac{\pi k_1}{L}x_1\right)\sin\left(\frac{\pi k_2}{L}x_2\right) \equiv \hat{\mathcal{F}}[\mathcal{X}(x_1,x_2)], \tag{A6}$$

$$\mathcal{X}(x_1,x_2) = \sqrt{\frac{2}{L}}\sum_{k_1=1}^{+\infty}\sum_{k_2=1}^{+\infty}\tilde{\mathcal{X}}(k_1,k_2)\sin\left(\frac{\pi k_1}{L}x_1\right)\sin\left(\frac{\pi k_2}{L}x_2\right) \equiv \hat{\mathcal{F}}^{-1}[\tilde{\mathcal{X}}(k_1,k_2)] \tag{A7}$$

by using the relation $\int_0^L dx\,\sin(\pi kx/L)\sin(\pi k'x/L) = L\delta_{kk'}/2$, $k = 1,2,\ldots$, $k' = 1,2,\ldots$ etc. Using Eq. (A7) we obtain

$$\hat{K}\mathcal{X}(x_1,x_2) = \hat{\mathcal{F}}^{-1}[\tilde{K}(k_1,k_2)\tilde{\mathcal{X}}(k_1,k_2)] \tag{A8}$$

with the kinetic operator $\hat{K} \equiv -[1/(2m)](\partial^2/\partial x_1^2 + \partial^2/\partial x_2^2)$ and the function $\tilde{K}(k_1,k_2) \equiv [\pi^2/(2mL^2)](k_1^2+k_2^2)$ of $k_1$ and $k_2$.

We discretize the time by a positive constant $\delta t$, so $t \to \nu\delta t, \nu = 0,1,2,\ldots$. By using the formal solutions of the Schrödinger equation, the wave function $\Psi(x_1,x_2,t+\delta t)$ at time $t+\delta t$ is related to the wave function $\Psi(x_1,x_2,t)$ at time $t$ as

$$\Psi(x_1,x_2,t+\delta t) = e^{-i\hat{H}\delta t/\hbar}\Psi(x_1,x_2,t) \tag{A9}$$

$$= e^{-iU(x_1,x_2)\delta t/(2\hbar)}e^{-i\delta t\hat{K}/\hbar}e^{-iU(x_1,x_2)\delta t/(2\hbar)} \times \Psi(x_1,x_2,t) + \mathcal{O}(\delta t^2) = e^{-iU(x_1,x_2)\delta t/(2\hbar)}\hat{\mathcal{F}}^{-1}[e^{-i\delta t\tilde{K}(k_1,k_2)/\hbar}\hat{\mathcal{F}} \times [e^{-iU(x_1,x_2)\delta t/(2\hbar)}\Psi(x_1,x_2,t)]] + \mathcal{O}(\delta t^2) \tag{A10}$$

where we used the relation (A8) and the boundary conditions $\Psi(0,x_2,t) = \Psi(x_1,0,t) = \Psi(L,x_2,t) = \Psi(x_1,L,t) = 0$ for the wave function of the system used in this paper. By Eq. (A10) we can calculate the wave function $\Psi(x_1,x_2,t+\delta t)$ at time $t+\delta t$ from the wave function $\Psi(x_1,x_2,t)$ at the previous time $t$.

An advantage of the pseudo-spectral method (A10) is that in this method we do not have to apply the space-differential operator $e^{-i\hat{H}\delta t/\hbar}$ in the time-evolution of wave function, and it is replaced by simple multiplications of just the numbers $e^{-iU(x_1,x_2)\delta t/(2\hbar)}$ and $e^{-i\delta t\tilde{K}(k_1,k_2)/\hbar}$, leading to less complicate numerical calculations than to use Eq. (A9) directly. Instead, we need to do a Fourier transformation and an inverse Fourier transformation for one step of the time evolution, but we can use the technique called by the fast Fourier transformation [34] in actual numerical calculations. The fast Fourier transformation requires the calculation time proportional to be $\tilde{\mathcal{N}}\log_2\tilde{\mathcal{N}}$ (instead of $\tilde{\mathcal{N}}^2$) for the total ($x_1x_2$ space) site number $\tilde{\mathcal{N}}$, and it is a big advantage for a fast numerical calculation of large $\tilde{\mathcal{N}}$ systems such as used in this paper.

## APPENDIX B: SURVIVAL PROBABILITY OF FREE PARTICLE SYSTEMS IN THE SEMI-INFINITE ONE-DIMENSIONAL SPACE

In this appendix we calculate the survival probability analytically for free particle systems in a semi-infinite one-dimensional space. First, we calculate it for the case of one free particle, and show analytically an asymptotic power decay (4) of the survival probability $P(t)$. Secondly, we show the different power decay behaviors (7) and (9) of the survival probabilities between two identical free bosons and fermions with the quantum effect of identity of two particles, such as the Pauli exclusion principle for fermions, in a semi-infinite one-dimensional space.

### 1. One-free-particle case

For one free particle in a one-dimensional space, the Hamiltonian operator is given by $\hat{H} = -[\hbar^2/(2m)]\partial^2/\partial x^2$. Then the wave function $\Psi'(x,t)$ for this Hamiltonian system in the full one-dimensional infinite region $(-\infty,+\infty)$ is represented as [45]

$$\Psi'(x,t) = \sqrt{\frac{m}{2\pi i\hbar t}} \int_{-\infty}^{+\infty} dy\ \Psi'(y,0) \exp\left[\frac{im(x-y)^2}{2\hbar t}\right] \tag{B1}$$

for any initial wave function $\Psi'(x,0)$ of the system. Using this function $\Psi'(x,t)$, the wave function $\Psi(x,t)$ for the system with the same Hamiltonian but in the semi-infinite one-dimensional region $[0,+\infty)$ is given by

$$\Psi(x,t) = \Xi'(t)^{-1}[\Psi'(x,t) - \Psi'(-x,t)] \tag{B2}$$

$$= \sqrt{\frac{m}{2\pi i\hbar t}} \int_{-\infty}^{+\infty} dy\ \Psi(y,0) \exp\left[\frac{im(x-y)^2}{2\hbar t}\right] \tag{B3}$$

for $x \geqslant 0$, so that the boundary condition $\Psi(0,t) = 0$ in the hard wall at $x = 0$ is automatically satisfied at any time $t$ by Eq. (B2). Here, $\Xi'(t) \equiv \int_0^{+\infty} dx\ |\Psi'(x,t) - \Psi'(-x,t)|^2$ is the quantity for normalizing the wave function $\Psi(x,t)$ as $\int_0^{+\infty} dx\ |\Psi(x,t)|^2 = 1$ for the semi-infinite space $[0,+\infty)$, and the initial wave function $\Psi(x,0) = \Xi'(0)^{-1}[\Psi'(x,0) - \Psi'(-x,0)]$ satisfies the condition $\Psi(-x,0) = -\Psi(x,0)$ for any real number $x$ in Eq. (B3). By using Eq. (B3) and noting the fact that the value of the initial wave function $\Psi(x,0)$ is 0 for $|x| > l$, the wave function $\Psi(x,t)$ of one free particle in the semi-infinite region $[0,+\infty)$ is represented as

$$\Psi(x,t) = \int_0^l dy\ G(x,y;t)\Psi(y,0) \tag{B4}$$

at position $x$ at time $t$, with $G(x,y;t)$ defined by

$$G(x,y;t) = \sqrt{\frac{m}{2\pi i\hbar t}} \left\{ \exp\left[\frac{im(x-y)^2}{2\hbar t}\right] - \exp\left[\frac{im(x+y)^2}{2\hbar t}\right] \right\}, \tag{B5}$$

as the time-evolutional propagator for one free particle in the semi-infinite one-dimensional space $[0,+\infty)$.

For large $t$ we expand the propagator $G(x,y;t)$ as

$$G(x,y;t) = -\sqrt{\frac{2i}{\pi}} \left(\frac{m}{\hbar t}\right)^{3/2} xy + \mathcal{O}(t^{-5/2}) \tag{B6}$$

up to the smallest nonzero order of $t^{-1}$. Inserting Eq. (B6) into Eq. (B4) and then calculating the survival probability, Eq. (3), for $N = 1$, we obtain Eq. (4) with coefficient (5).

### 2. Two-identical-free-particle cases

We consider a two-identical-free-particle system with no potential energy in a semi-infinite one-dimensional space. In this case, because there is no potential energy, the time evolution of the wave function $\Psi(x_1,x_2,t)$ of this system is dominated by the one-particle propagator (B5) and is given by

$$\Psi(x_1,x_2,t) = \int_0^l dy_1 \int_0^l dy_2 G(x_1,y_1;t)G(x_2,y_2;t)\Psi(y_1,y_2,0). \tag{B7}$$

Here, we used the fact that values of the wave function $\Psi(y_1,y_2,0)$ at initial time $t = 0$ are nonzero only in the region satisfying $0 < y_1 < l$ and $0 < y_2 < l$ as assumed in this paper.

Now, we impose the condition

$$\Psi(x_2,x_1,0) = \pm\Psi(x_1,x_2,0), \tag{B8}$$

that is, condition (6) at initial time $t = 0$. Here, the plus sign (minus sign) on the right-hand side of Eq. (B8) is taken for identical bosons (fermions). Under condition (B8), wave function (B7) automatically satisfies condition (6) at any time $t$. We can rewrite Eq. (B7) using Eq. (B8) as

$$\Psi(x_1,x_2,t) = \frac{1}{2}[\Psi(x_1,x_2,t) \pm \Psi(x_2,x_1,t)]$$

$$= \frac{1}{2}\int_0^l dy_1 \int_0^l dy_2 [G(x_1,y_1;t)G(x_2,y_2;t) \pm G(x_2,y_1;t)G(x_1,y_2;t)]\Psi(y_1,y_2,0), \tag{B9}$$

so that the wave function $\Psi(x_1,x_2,t)$ automatically satisfies condition (6) at any time $t$ without noting condition (B8) anymore.

#### *a. Boson case*

For the system consisting of two identical free bosons, by Eq. (B6) the quantity $G(x_1,y_1;t)G(x_2,y_2;t) + G(x_2,y_1;t)G(x_1,y_2;t)$ is asymptotically represented as

$$G(x_1,y_1;t)G(x_2,y_2;t) + G(x_2,y_1;t)G(x_1,y_2;t) = \frac{4i}{\pi}\left(\frac{m}{\hbar t}\right)^3 x_1x_2y_1y_2 + \mathcal{O}(t^{-4}). \tag{B10}$$

Inserting Eq. (B10) into Eq. (B9) and then calculating the survival probability (3) for $N = 2$, we obtain Eq. (7) with coefficient (8).

***b. Fermion case***

For a system consisting of two identical free fermions we expand the one-particle propagator, Eq. (B5), as

$$G(x,y;t) = \sqrt{\frac{2i}{\pi}}\left(\frac{m}{\hbar t}\right)^{3/2} xy\left[1 + \frac{im}{2\hbar t}(x^2+y^2) - \frac{1}{24}\left(\frac{m}{\hbar t}\right)^2 \times (3x^2 + 10x^2y^2 + 3y^2) + \mathcal{O}(t^{-3})\right] \tag{B11}$$

up to the order $t^{-7/2}$, which is a higher order than in Eq. (B6). By Eq. (B11) the quantity $G(x_1,y_1;t)G(x_2,y_2;t) - G(x_2,y_1;t)G(x_1,y_2;t)$ is asymptotically represented as

$$G(x_1,y_1;t)G(x_2,y_2;t) - G(x_2,y_1;t)G(x_1,y_2;t) = \frac{1}{3\pi i}\left(\frac{m}{\hbar t}\right)^5 x_1x_2y_1y_2\left(x_1^2 - x_2^2\right)\left(y_1^2 - y_2^2\right) + \mathcal{O}(t^{-6}). \tag{B12}$$

Inserting Eq. (B12) into Eq. (B9) and then calculating the survival probability, Eq. (3), for $N = 2$, we obtain Eq. (9) with coefficient (10).


[1] H. Risken, *The Fokker-Planck Equation: Methods of Solution and Applications* (Springer-Verlag, Berlin, 1989).

[2] N. G. van Kampen, *Stochastic Processes in Physics and Chemistry* (Elsevier, Amsterdam, 1992).

[3] P. Hänggi, P. Talkner, and M. Borkovec, Rev. Mod. Phys. **62**, 251 (1990).

[4] R. W. Gurney and E. U. Condon, Phys. Rev. **33**, 127 (1929).

[5] R. G. Winter, Phys. Rev. **123**, 1503 (1961).

[6] W. van Dijk and Y. Nogami, Phys. Rev. Lett. **83**, 2867 (1999); Phys. Rev. C **65**, 024608 (2002).

[7] H. J. Kupka, *Transitions in Molecular Systems* (Wiley-VCH, Weinheim, 2010).

[8] E. G. Altmann and T. Tél, Phys. Rev. Lett. **100**, 174101 (2008); Phys. Rev. E **79**, 016204 (2009).

[9] V. Paar and H. Buljan, Phys. Rev. E **62**, 4869 (2000).

[10] L. A. Bunimovich and C. P. Dettmann, Phys. Rev. Lett. **94**, 100201 (2005).

[11] P. Gaspard and G. Nicolis, Phys. Rev. Lett. **65**, 1693 (1990).

[12] P. Gaspard, *Chaos, Scattering and Statistical Mechanics* (Cambridge University Press, Cambridge, 1998).

[13] R. Klages, *Microscopic Chaos, Fractals and Transport in Nonequilibrium Statistical Mechanics* (World Scientific, Singapore, 2007).

[14] S. Datta, *Electronic Transport in Mesoscopic Systems* (Cambridge University Press, Cambridge, 1995).

[15] Y. Imry, *Introduction to Mesoscopic Physics* (Oxford University Press, New York, 1997).

[16] W. Bauer and G. F. Bertsch, Phys. Rev. Lett. **65**, 2213 (1990); O. Legrand and D. Sornette, *ibid.* **66**, 2172 (1991); W. Bauer and G. F. Bertsch, *ibid.* **66**, 2173 (1991).

[17] H. Alt, H.-D. Gräf, H. L. Harney, R. Hofferbert, H. Rehfeld, A. Richter, and P. Schardt, Phys. Rev. E **53**, 2217 (1996).

[18] L. A. Bunimovich and C. P. Dettmann, Europhys. Lett. **80**, 40001 (2007).

[19] V. Milner, J. L. Hanssen, W. C. Campbell, and M. G. Raizen, Phys. Rev. Lett. **86**, 1514 (2001).

[20] N. Friedman, A. Kaplan, D. Carasso, and N. Davidson, Phys. Rev. Lett. **86**, 1518 (2001).

[21] M. F. Demers and L.-S. Young, Nonlinearity **19**, 377 (2006).

[22] J.-W. Ryu, S.-Y. Lee, C.-M. Kim, and Y.-J. Park, Phys. Rev. E **73**, 036207 (2006).

[23] S. Shinohara and T. Harayama, Phys. Rev. E **75**, 036216 (2007).

[24] T. Tél and M. Gruiz, *Chaotic Dynamics: An Introduction Based on Classical Mechanics* (Cambridge, New York, 2006).

[25] M. Miyamoto, Phys. Rev. A **68**, 022702 (2003).

[26] A. del Campo, F. Delgado, G. García-Calderón, J. G. Muga, and M. G. Raizen, Phys. Rev. A **74**, 013605 (2006).

[27] G. García-Calderón, I. Maldonado, and J. Villavicencio, Phys. Rev. A **76**, 012103 (2007).

[28] C. H. Lewenkopf and H. A. Weidenmüller, Ann. Phys. (NY) **212**, 53 (1991).

[29] F.-M. Dittes, H. L. Harney, and A. Müller, Phys. Rev. A **45**, 701 (1992); H. L. Harney, F.-M. Dittes, and A. Müller, Ann. Phys. (NY) **220**, 159 (1992).

[30] I. V. Zozoulenko and T. Blomquist, Phys. Rev. B **67**, 085320 (2003).

[31] Exactly speaking, for example, the plus sign in the plus or minus sign on the right-hand side of Eq. (2) can be taken even for fermions if the wave function is represented as a multiplication of a spatially dependent part and a spin-dependent part, and its spin-dependent part is antisymmetric for exchange of any two particles. However, in this paper we do not consider such a spin effect.

[32] The term "survival probability" has been used in some reports, such as Refs. [18–20] and [30] and comes from the fact that $P(t)$ is the probability that particles will "survive" within the subspace at time $t$. However, it should also be noted that in some papers, like Refs. [6] and [25–27], a quantity like Eq. (3) is called the "nonescape probability," and the term survival probability is used for a slightly different quantity.

[33] M. D. Feit, J. A. Fleck Jr., and A. Steiger, J. Comput. Phys. **47**, 412 (1982).

[34] P. L. DeVries and J. E. Hasbun, *A First Course in Computational Physics* (Jones and Bartlett, Sudbury, MA, 2011).

[35] A. J. Fendrik, M. J. Sánchez, and P. I. Tamborenea, Phys. Rev. B **63**, 115313 (2001).

[36] In actual numerical calculations, the spatial integrals in Eqs. (13) and (14) are replaced by sums of $|\Psi_n(x,x_2,t)|^2$ over spatially discretized sites of $x_2$, and the contribution of $|\Psi_n(x,x_2,t)|^2$ at the same site $x_2 = x$ for the two particles in these sums is taken as its half, so that relation (15) is still satisfied even in this spatially discretized case. We also note that the distributions $f_n^{(R)}(x,t)$

and $f_n^{(L)}(x,t)$ defined by Eqs. (13) and (14), are normalized as $\int_0^{+\infty} dx\ f_n^{(R)}(x,t) = \int_0^{+\infty} dx\ f_n^{(L)}(x,t) = 1/2$.

[37] Concretely speaking, to calculate the survival probabilities shown in Fig. 12 we chose the classical initial ensemble of particles given by the following three process. (i) We first pick up the particle positions $x_1$ and $x_2(>x_1)$ uniformly from the spatial area in which values of the potential energy $U(x_1,x_2)$ defined by Eq. (11) are lower than $E_n$. (ii) We calculate the kinetic energy $K = E_n - U(x_1,x_2)$ for each point $(x_1,x_2)$ given in process i. (iii) We pick up the particle momenta $p_1$ and $p_2$ of two particles uniformly from the circle $p_1^2 + p_2^2 = 2mK$ with the kinetic energy $K$ calculated in process ii. In these numerical calculations of the survival probabilities in Fig. 12, we also used an approximation in which the contribution of particles to the survival probability $P_n(t)$ after one of two particles has escaped from the subsystem is negligible.

[38] M. C. Gutzwiller, *Chaos in Classical and Quantum Mechanics* (Springer-Verlag, New York, 1990).

[39] E. Ott, *Chaos in Dynamical Systems* (Cambridge University Press, Cambridge, 1993).

[40] H.-J. Stöckmann, *Quantum Chaos: An Introduction* (Cambridge University Press, Cambridge, 1999).

[41] F. Selva and J.-L. Pichard, Eur. Phys. J. B **20**, 441 (2001).

[42] P. S. Drouvelis, P. Schmelcher, and F. K. Diakonos, Phys. Rev. B **69**, 035333 (2004).

[43] S. Sawada, A. Terai, and K. Nakamura, Chaos Solitons Fractals **40**, 862 (2009).

[44] S. E. Ulloa and D. Pfannkuche, Superlattices Microstruct. **21**, 21 (1997).

[45] R. P. Feynman and A. R. Hibbs, *Quantum Mechanics and Path Integrals* (McGraw-Hill, New York, 1965).